J Polym Res (2015) 22: 207
DOI 10.1007/s10965-015-0844-x

ORIGINAL PAPER

Preparation of superhydrophobic and self-cleaning polysulfone non-wovens by electrospinning: influence of process parameters on morphology and hydrophobicity

M. Al-Qadhi[1] · N. Merah[1,2] · A. Matin[2,4] · N. Abu-Dheir[1] · M. Khaled[3] · K. Youcef-Toumi[5]

Received: 6 May 2015 / Accepted: 11 September 2015 / Published online: 6 October 2015

Abstract Electrospinning is used to prepare hydrophobic and self-cleaning polysulfone (PSf) surfaces. The effects of PSf concentration in Dimethylformamide (DMF) solvent and electrospinning process parameters on the surface structure and hydrophobicity are investigated. The experimental results show that depending on PSf concentration, three types of morphologies are obtained: beads, beads-on-strings, and free-beads fibers. The surface hydrophobicity depends mainly on the resultant surface morphology, and the existence of beads increases hydrophobicity. The contact angle (CA) is found to increase from 73° for smooth PSf surface to more than 160° for surfaces formed by electrospinning. Moreover, the contact angle hysteresis (CAH) was generally less than 10° for all the chemistries. It is noted that increasing the PSf concentration leads to the formation of beads-on-string and free-beads fiber structures; this morphological change is accompanied by a reduction in the contact angle. Surface structures are found to be more sensitive to electrospinning feed rate than to electrospinning voltage; however, these two parameters have a negligible influence on the hydrophobicity. Porosity measurements of different chemistries show an average pore size in the range 3–8 microns. The thickness of PSf mats was variable, from as low as 10 μm to as high as 70 μm.

Keywords Electrospinning · Polysulfone · Superhydrophobic · Fiber structures

✉ A. Matin
amatin@kfupm.edu.sa

[1] Department of Mechanical Engineering, King Fahd University of Petroleum and Minerals, Dhahran 31261, Saudi Arabia

[2] Center of Excellence for Scientific & Research Collaboration with MIT, King Fahd University of Petroleum and Minerals, Dhahran 31261, Saudi Arabia

[3] Department of Chemistry, King Fahd University of Petroleum and Minerals, Dhahran 31261, Saudi Arabia

[4] Center for Engineering Research, King Fahd University of Petroleum and Minerals, Dhahran 31261, Saudi Arabia

[5] Department of Mechanical Engineering, Massachusetts Institute of Technology, Cambridge, MA 01239, USA

Introduction

Superhydrophobic surfaces with water contact angle (CA) higher than 150° are expected to have extensive applications in self-cleaning surfaces, protective clothes, anti-biofouling, prevention of water corrosion, anti-contamination fields, oil–water separation, and anti-sticking and microfluidic systems [1–3]. Self-cleaning surfaces are hydrophobic surfaces that havea a high contact angle; hence, with small tilt angle or under tiny disturbance, a spherical water droplet can roll off the surface. Due to the surface tension, dust particles tend to adhere to the water droplet during rolling off and can be removed easily from the surface [1]. Research on self-cleaning surfaces has been attracting more and more attention after Neinhuis and Barthlott [4] revealed that the reason behind the self-cleaning properties of lotus flowers was the epicuticular wax crystalloids of the surface. In fact, the hydrophobicity of materials depends on their surface energy and the surface roughness. For native surfaces, the highest CA that can be achieved for lowest surface energy is 120° [for Trifluoromethyl (CF_3) groups] [2, 5] . However, surfaces with CAs higher than 150° can be achieved by controlling the surface roughness. Once the components of materials have been chosen, surface roughness is the key factor that determines the hydrophobicity of the surfaces. A number of methods were employed to fabricate and control the surface

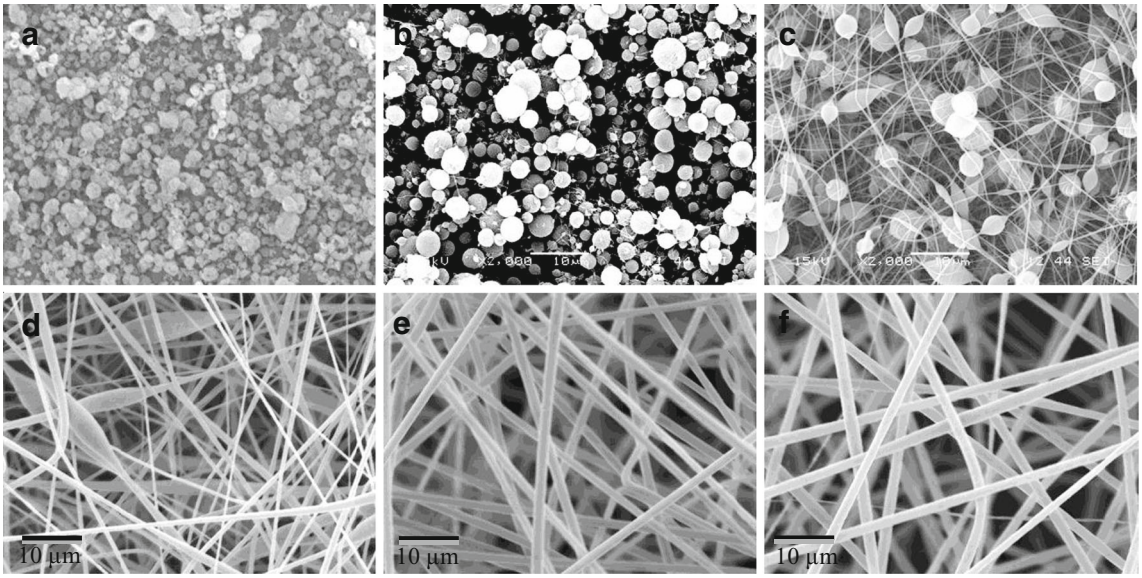

Fig. 1 SEM micrographs of electrospun samples prepared using different PSf concentration (X2000): **a**) 5 wt%, **b**) 10 wt%, **c**) 15 wt%, **d**) 20 wt%, **e**) 25 wt%, and f) 30 %

roughness, including; lithography, chemical vapor deposition (CVD), polymer reconformation, sublimation, electrospinning, plasma technique, sol–gel processing, electrodeposition, hydrothermal synthesis, and layer-by-layer methods [1]. As a result of their high surface roughness, films fabricated from micro and nanofiber morphologies are shown to have high CAs [5–8].

Different approaches are used to synthesize micro and nanofibers; electrospinning is one of the most versatile techniques used to roughen surfaces [6–9]. Due to its low cost, applicability to a wide range of materials, and ability to produce fibers with diameters ranging from scores of nanometers to several micrometers, electrospinning has attracted more attention for academic studies and industrial applications [3, 9, 10]. The electrospinning process, and hence the morphologies of fabricated fibers, depends on several solution parameters, including molecular weight, concentration, viscosity, surface tension, and electrical conductivity, as well as electrospinning conditions such as voltage, feed rate and distance between the nozzle and collector [6, 9, 11]. Zheng et al. [2] studied the effect of solution properties and electrospinning parameters on the surface morphology using polystyrene (PS). They found that the contact angles for PS fiber morphologies were between 140° and 150°, while the CAs of particle structures reached 160°. Wang et al. [3] prepared thermoplastic polyurethane (TPU) mats with bead-on-string structure using electrospinning. Their study showed that a resultant contact angle of 150° could be obtained after surface treatment with hydrophobic nanosilicas. Jiang et al. [6] were able to fabricate a superhydrophobic PS film with morphologies of both porous microspheres and nanofiber using an electrospinning process. Chen and Kim [7] used electrospinning to fabricate poly(vinylidene fluoride) (PVDF) superhydrophobic membranes with a CA higher than 150°.

Electrospinning of Polysulfone (PSf) is traditionally used to prepare membranes that are light in weight and excellent in permeability [10, 11]. However, to the best of our knowledge, preparation of superhydrophobic and self-cleaning polysulfone surfaces by electrospinning has not yet been reported in literature. Therefore, the primary objective of this study was to synthesize such surfaces, and then to study the influence of polysulfone concentration on surface morphology and hydrophobicity. The influence of electrospinning feed rate and electrospinning voltage on the structure of prepared PSf surfaces was also examined. Scanning electron microscope was used to determine the morphologies of the fabricated films and the hydrophobicity was determined by measuring the contact angle.

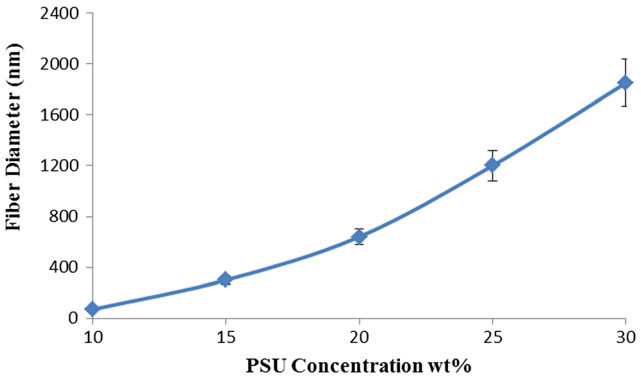

Fig. 2 Variation of average fiber diameter with polysulfone concentration

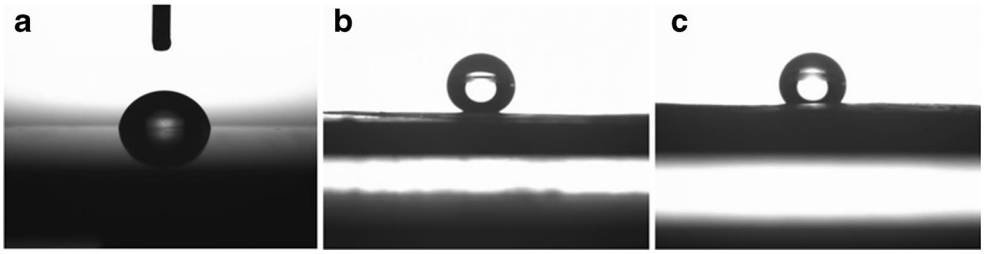

Fig. 3 Images showing the behavior of water droplets on: **a)** splashed layer of PSf (CA=73°) and electrospun PSf surfaces prepared from different PSf concentrations: **b)** 5 wt% (CA=160°), and **c)** 30 wt% (CA=135°)

Materials and experiments

Materials

Polysulfone (PSf) with an average molecular weight of 35,000 (g/mol) supplied by BOC Sciences was dissolved in N,N-Dimethylformamide (DMF) with 0.944 (g/cm^3) density, supplied by Alfa Aesar. PSf concentrations ranging from 5 to 30 % were considered. These materials were used without any further modification or purification. For preparing the electrospun mats for further characterization, the samples were etched using Keller's reagent, which is a mixture of DI water and three different acids, in the following ratios: 95 mL water, 2.5 mL HNO_3, 1.5 mL HCI, 1.0 mL HF.

Electrospinning process

The preparation of PSf solution started by dissolving required amounts of PSf in DMF at 40 °C using a magnetic stirrer. The magnetic mixing continued for 6 hours until a uniform and homogenous solution (transparent solution) was obtained. To investigate the effect of PSf concentration on the resultant morphology and hence surface hydrophobicity, solutions with six different concentrations (5, 10, 15, 20, 25, and 30 wt% of PSf in DMF) were prepared. A required amount of the PSf solution was fed into a syringe (5 ml) with a metal spinneret having an inner diameter of 0.6 mm. The syringe was fixed inside the electrospinning chamber before starting to adjust the parameters of the NANON Electrospinning apparatus (MECC Ltd., Japan). The operating voltage of this machine was between 0 and 30 kV with a maximum distance of 150 mm between spinneret and collector. In this work, six different feed rates (0.4, 0.8, 1.3, 2, 2.5, and 3.5 ml/h) were used, and the applied voltage was adjusted so that stable Taylor cone was achieved. The electrospinning voltage that achieves optimum stable Taylor cone depends on PSf concentration and feed rate; the electrospinning voltage used here was between 17 and 26 kV. The distance between needle and the collector was kept constant at 150 mm. This distance was found to be the best distance to produce uniform electrospun structure [11].

Characterization of surfaces

The morphology of the electrospun PolySulfone mats and the general features of the fibers were investigated using scanning electron microscopy (SEM, TSM-6460). Prior to analysis, the specimens were sputter-coated with a 5–6 nm layer of gold with a Desk II cold sputter/etch unit (Denton Vacuum LLC). The images were taken at different magnifications and from different regions of the samples to obtain a complete picture. The average fiber diameter was estimated from the images at relatively higher magnifications.

The water contact angles of the electrospun surfaces were measured using a goniometer model DM-501 (Kyowa Interface Science Co. Ltd., Japan) equipped with FAMAS software. For measuring the static angles, the sessile drop method was utilized, with a droplet size of about 20 μl. Five to six measurements were carried out for each sample from different locations and the average value taken. Dynamic angles were measured using the extraction/retraction method for the advancing and receding angles. For each measurement, 48 values were recorded and the same number of images captured.

Porosity is an important parameter for electrospun fibers, as it ultimately influences the surface roughness, and hence, hydrophobicity. Traditionally, mats produced by electrospinning are quite porous, with 70–80 % of the surface area being empty spaces. A mercury porosimeter was utilized to determine the porous characteristics of the PSf mats. The mean

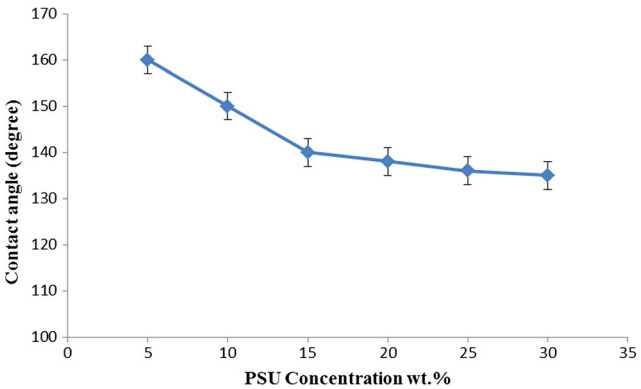

Fig. 4 The effect of polysulfone concentration on the contact angle of the resultant structure

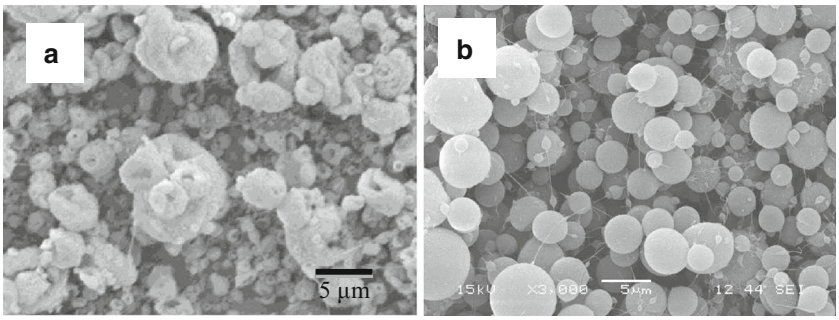

Fig. 5 SEM micrographs of electrospun samples showing the roughness of the beads for samples prepared using different PSf concentrations: **a**) 5 % (CA=160°) and **b**) 10 % (CA=150°) (X3000)

pore size and other relevant parameters were calculated by the software of the instrument. By using a pair of very fine tweezers, the mats were carefully removed from the glass and placed on the specimen holder.

The thickness of the polysulfone mats was measured using a simple table-top LITEMATIC VL-50A. This consists of a small stage on which the sample is placed and a movable indenter that makes contact with the surface. Virgin glass slides were used as the reference material.

Results and discussion

It is known that the morphology of fabricated hydrophobic surfaces depends on the viscosity, the surface tension and the thermal conductivity of the solutions, and the electrospinning parameters [5, 10–12]. Some of the effects of these parameters are investigated in the following.

Solution concentration

Solution concentration is the main factor affecting the electrospinning process, and hence, controlling the resultant morphology. Too high a concentration will hinder the solution from being pumped, however, very low concentration will lead to breakdown of the jet due to the low amount of polymer chain entanglements, that is, low viscosity [13, 14]. The effects of solution concentration on the resultant morphology of the fabricated PSf surfaces are illustrated in Fig. 1. The figure shows SEM micrographs of electrospun PSf surfaces prepared from solutions containing different concentrations of PSf in DMF. During the fabrication of these samples, electrospinning feed rate and voltage were kept constant at 1.3 ml/h and 22 kV, respectively. Three types of PSf surface morphologies were formed: beads structure, beads-on-string structure, and free-beads fiber structure. The beads structure shown in Fig. 1a was prepared from a solution containing 5 wt% of PSf, while the beads-on-strings morphologies shown in Fig. 1b, c, and d were fabricated from solutions with 10 wt%, 15 wt% and 20 wt% of PSf, respectively.

The formation of bead structures from the diluted solution (5 wt% of PSf) can be attributed to the low viscosity of the solution due to the fewer chain entanglements and the higher amount of solvent [5, 6]. In fact, for low concentration solution and hence low viscosity, the high surface tension overcomes the viscosity, which leads to the formation of beads. Combination of half-hollow beads and beads having a collapsed surface with an average bead size of about 2.5 μm were produced. When the solution concentration of PSf increased to 10 wt%, the resultant morphology was a combination of microspheres and nanofibers, as shown in Fig. 1b. The average size of microspheres was about 2.9 μm and the nanofibers have an average diameter about 70 nm. For solutions with 15 wt% of PSf, beads-on-string structures were obtained as displayed in Fig. 1c. The average size of the beads was about 3.6 μm and the average fibers diameter was about 300 nm. The shape of beads changed from spherical to spindle-like when increasing PSf concentration to 20 wt%, as illustrated in Fig. 1d. In this case, a smaller number of beads was observed and the average beads and fibers diameters were about 2.5 μm and 640 nm, respectively. When the solution concentration exceeded 20 wt%, free-beads fibers resulted, as shown in Fig. 1f and g. The average fibers diameters for samples fabricated from solutions with 25 wt% and 30 wt% of PSf were 1.2 μm and 1.85 μm, respectively.

The absence of beads with increasing PSf concentration can be attributed to the high viscosity of the solution, and hence a higher number of chain entanglements that will keep the continuity of fibers and overcome the surface tension during the electrospinning process. It is also clear that increasing

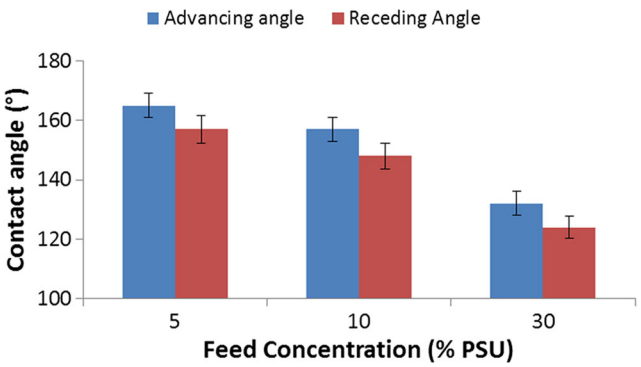

Fig. 6 Average values of the advancing (*blue*) and receding (*red*) angles for three different chemistries

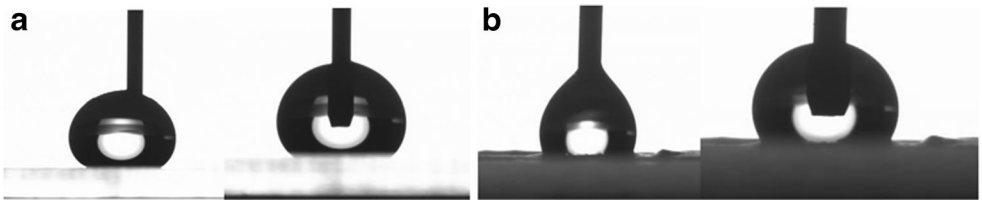

Fig. 7 Images of water droplets on (**a**) 10 % PSf and (**b**) 30 % PSf during dynamic measurements. The left hand side image is of the advancing angle, whereas the right hand side is for the receding angle

the solution concentration leads to an increase in the average diameter of the fibers, as illustrated in Fig. 2. The average fiber diameter increased with PSf concentration according to the second power law. A number of studies were carried out on the effect of concentration on fiber diameter [11, 12, 14]; some reported that the average fiber diameter increased linearly with concentration [11, 12], while others found that the average fiber diameter increased with concentration according to the third power low [14].

The hydrophobicity of the fabricated surface morphology was investigated by measuring the resulting contact angles. Compared with a native PSf layer splashed on aluminum foil, which has a CA about 73°, the CAs of PSf surfaces fabricated by electrospinning process are twice as high as illustrated in Fig. 3. The highest CA was 160° for PSf surfaces prepared from a solution with 5 % concentration with the beads morphology (Fig. 3b), while the lowest CA was 135° for samples fabricated from a solution with 30 wt% (Fig. 3c), which was seen to have free-bead fibers structure. Figure 4 shows that the contact angle increases rapidly with decreasing concentration of PSf below 15 wt%. This is mainly associated with the presence of beads, as is evident from Fig. 1 a–c. The absence of bead structure, for concentrations higher than 15 wt%, resulted in lower CAs with limited effect of PSf concentration.

This change in the hydrophobicity of the prepared surfaces can be attributed to the morphological change of the surface structure. In fact, the change in the surface wettability can mainly be related to the contact area between the water droplet and the solid surface, which depends on the surface roughness [1, 15]. The air trapped in the apertures within the rough surface is responsible for increasing the hydrophobicity, since the water contact angle of air is considered to be around 180°. Cassie and Baxter [16] suggested Equation (1) to describe the relationship between water droplet CA on a smooth surface (θ) and water droplet CA on a rough surface (θ_r) composed of a solid and air.

$$\cos\theta_r = f_1\cos\theta - f_2 \quad (1)$$

Where f_1 and f_2 are the fractions of solid surface and air that are in contact with the water droplet, respectively, $f_1+f_2=1$. Using the CAs of the smooth PSf surface and the free-beads fiber structure of PSf (for samples prepared from solution with 30 wt% of PSf), f_2 is found to be 0.77. This means that, about 77 % of the surface of free-beads fibers structure beneath the water droplet is air. This is clear from the SEM micrographs shown and from porosity in Fig. 1f, which indicate that the surface area of the fibers that will be in contact with the water droplet accounts for a small part of the total surface.

The variation in CA between samples fabricated with 25 and 30 wt% PSf concentrations is small (136° and 135°, respectively), due to the slight change in their morphologies. This is clear when comparing micrographs (e) and (f) of Fig. 1. The only change is the difference in fiber diameter; the sample prepared from solution with 30 wt% PSf concentration has higher diameter (Fig. 2). Higher diameter means more contact surface between water droplets and the PSf surface, and hence lower CA. With decreasing the PSf concentration, the resultant morphology changed from free-bead fiber structure (Fig. 1e) to bead-on-string structure (Fig. 1c); this morphological change was accompanied by an increase of CA from 136° to 141°. Similar results were reported in previous works where the bead-on-string morphology led to higher hydrophobic surfaces compared with free-bead fiber structures when using polystyrene (PS) [5, 6]. Zhan et al. [5] found that the contact angle for bead-on-string fibers was about 154.5°, compared to 146° for free-bead fibers.

At lower concentration (10 %, Fig. 1b) where the structure was dominated by microspheres with some nanofibers, the surfaces became superhydrophobic with CA around 150°. At the lowest concentration (5 %, Fig. 1a) in which the resultant morphology was microspheres, clear enhancement in the non-wettability was observed and the CA reached 160°. This

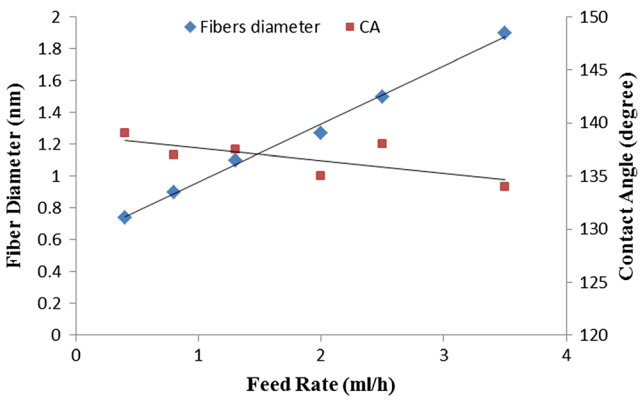

Fig. 8 Variation of average fiber diameter and contact angle with electrospinning feed rate for sample with 25 % PSf concentration

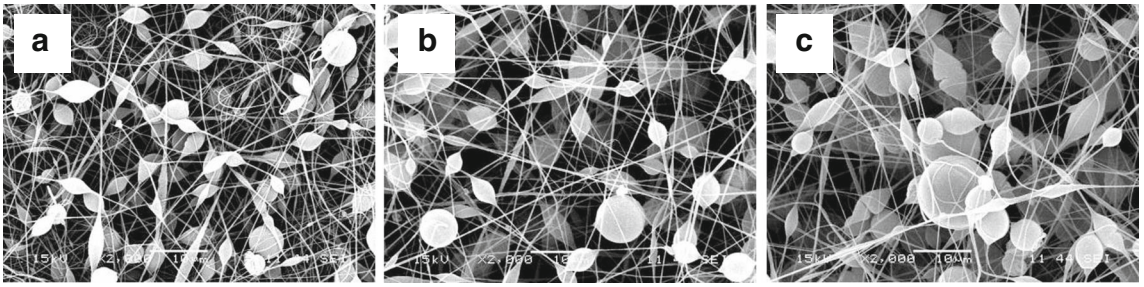

Fig. 9 SEM micrographs for electrospun PSf samples with 15 % concentration, showing the morphologies for samples fabricated with different feed rates: **a**) 0.8 ml/h, **b**) 2.5 ml/h, and **c**) 3.5 ml/h

improvement in the hydrophobicity for the sample with 5 % concentration compared 10 % can be attributed to the rougher surfaces of the microspheres for the sample with 5 %, as shown in Fig. 5.

Figure 4 shows a plot of the static water contact angle as a function of the polysulfone concentration in the feed solution. A similar behavior was also observed by Acatay et al. [17], who synthesized a copolymer made up of acrylonitrile (AN) and isopropenylbenzyl isocyanate (TMI) in DMF and then mixed the result with a perfluorinated linear diol. By varying the composition of the feed solution, they were able to prepare solutions of different viscosities. The resulting mats had different morphologies ranging from bead-only to continuous fibers. The measured static water contact angle was as high as 156° for the former, whereas it was below 150° for the latter.

The above observations can be explained as follows: a surface consisting of beads several microns in diameter (Fig. 5a, and b) can be rougher than a surface covered with fibers having an average thickness below 1 μm. Furthermore, the bead-rich topography increases the discontinuities in the triphasic contact line a lot more than a fibrous surface [18]. The triphasic contact line is defined as the boundary between three different surfaces: air, water and the specimen.

For a surface to be truly superhydrophobic, there are two requirements: a static angle in excess of 150°, and a contact angle hysteresis (CAH) of less than 10° [19]. Many surfaces appear to be superhydrophobic with the first condition satisfied [20–22] . However, due to the high adhesion and sticky nature of the surface, the water droplet is pinned to the surface [23], resulting in a large difference between the advancing and receding angles. Currently, there are only a few studies that also report low hysteresis or a low sliding angle of the water droplet [24–26].

In view of the above, it was deemed necessary to carry out dynamic contact angle measurements on the electrospun polysulfone mats. The procedure was typical: first touching the needle tip to the water droplet and measuring the advancing angles; then bringing the tip close to the sample surface and recording the receding angles. The results are presented in Fig. 6 as bar charts for certain selected compositions; 5, 10 and 30 % PSf. It is observed that the mean hysteresis values for all the chemistries lie in the range 5°<CAH <10°.

Figure 7 shows some representative images of the water droplets for two different chemistries, 10 % and 30 % PSf. The images correlate well with the above findings (Fig. 6) that the difference between the two angles is not significant. These findings are a good indicator of the stability of the superhydrophobic state of these surfaces, regardless of the chemical composition, which effectively determines the self-cleaning behavior as well [27, 28]. An interesting observation is that even surfaces that don't really qualify as superhydrophobic because of angles below 150°, have a substantially low CAH and may still be considered for self-cleaning applications. In fact, the mechanical integrity associated with the higher chemistries may make them a more viable option than the lower concentrations that were found to be very fragile.

In the literature, two different states are used to define the equilibrium for rough superhydrophobic surfaces: Cassie and Wenzel states. The Wenzel state exhibits a high water contact angle (WCA) owing to an increase in surface area, whereas the Cassie state describes a high WCA owing to trapped air pockets in the rough surface. The Cassie regime offers a lower hysteresis between advancing and receding WCAs, because the water droplet is mostly in contact with the trapped air, and the hydrophobic surface has a lower sliding (roll-off) angle.

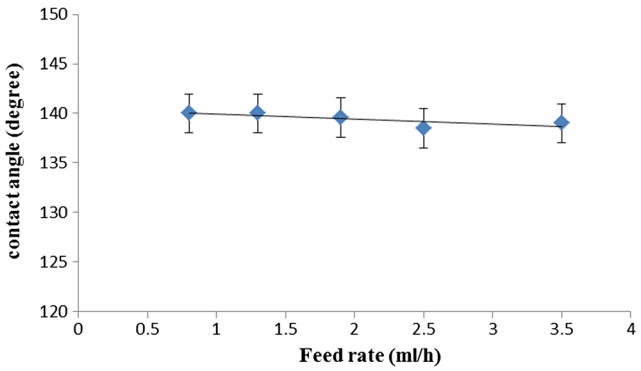

Fig. 10 Change of contact angle with electrospinning feed rate for samples prepared with 15 wt% PSf concentration

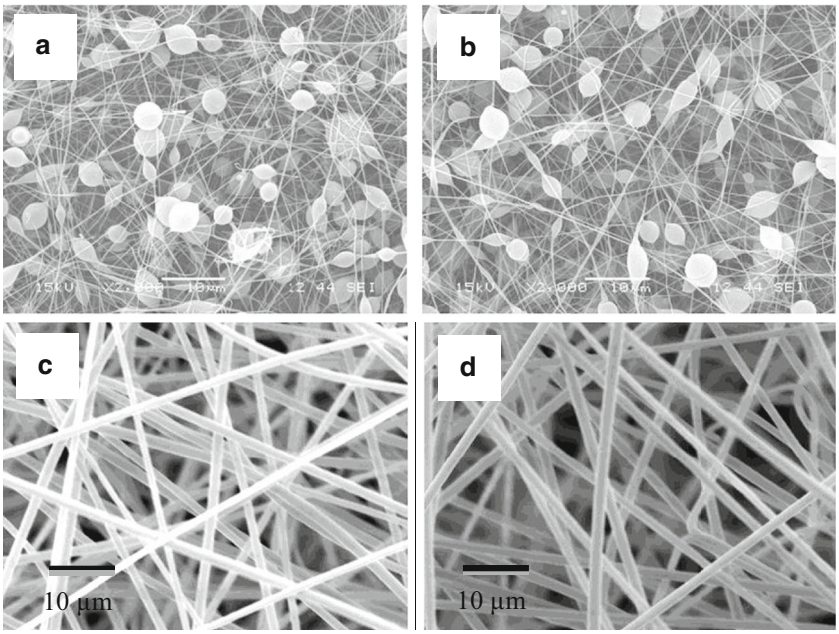

Fig. 11 SEM micrographs (X2000) for electrospun samples prepared at different electrospinning voltages for samples with 15 % PSf concentration: **a**) 17 kV, **b**) 24 kV and samples with 25 % of PSf: **c**) 20 kV, and d) 26 kV

Based on the above description, the PSf surfaces appear to be in a Cassie state of wetting.

Effect of electrospinning feed rate

The feed rate represents the amount of solution to be electrospun per time. It is one of the important electrospinning parameters that control the stability of Taylor cone. In this study, the feed rate was varied from 0.4 to 3.5 (ml/h). The average fibers diameter is found to increase with increasing electrospinning feed rate, as shown in Fig. 8. As can be seen in the figure, the average fibers diameter increased linearly from 0.74 μm for samples with 0.4 ml/h feed rate to 1.9 μm for samples fabricated with 3.5 ml/h. This increase in the fiber diameter is attributed to the shorter time taken for the jet to move from spinneret to collector, and hence, the smaller solvent evaporation rate, which leaves thicker fibers [11]. In addition, higher feed rate means greater amount of polymer chain entanglements, and hence thicker fibers. The variation of contact angle with feed rate for a solution with 25 wt% PSf concentration is also illustrated in Fig. 8. The CA is seen to decrease with increasing feed rate, and hence with increasing fiber diameter, resulting in larger contact area between water droplet and PSf surface.

For samples prepared from low concentration of PSf (10 & 15 %), the change in the resultant morphology with feed rate was diminished, as illustrated by the SEM micrographs in Fig. 9 for 15 wt% PSf. For this concentration, the change in the average fiber diameter with feed rate is negligible, while there is a clear increase in the average diameter of beads, which varied from 3 μm for samples synthesized with 0.8 ml/h feed rate to 5.5 μm for those synthesized with 2 ml/h. In this case, due to the negligible change of the resultant morphology with feed rate, the variation of contact angle with feed rate is insignificant, as shown in Fig. 10.

Influence of electrospinning voltage

In addition to the electrospinning feed rate, electrospinning voltage is another important parameter controlling the stability of Taylor cone. Using low voltage may not be enough to generate the required elongational force that is responsible for fiber thinning; on the other hand, high voltage may lead to instability of the jet at the spinneret in which the Taylor cone is receding. In this study, the electrospinning voltage was controlled to reach stable Taylor cone. It was found that within the range of 17 to 26 kV, it was possible to fabricate uniform surfaces. However, outside this range, the Taylor cone was unstable. It should also be noted that increasing the PSf concentration led to an increase in the optimum electrospinning voltage.

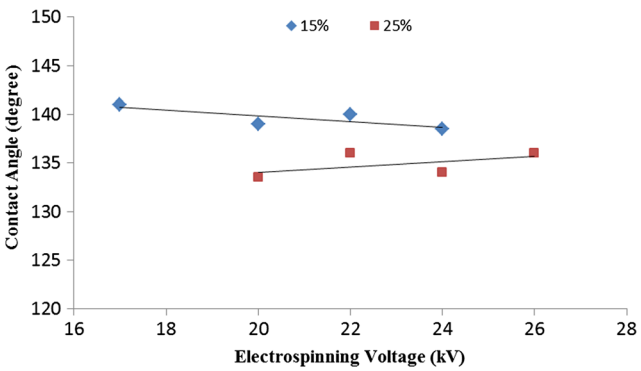

Fig. 12 Effect of electrospinning voltage on contact angle for samples with 15 % and 25 % PSf

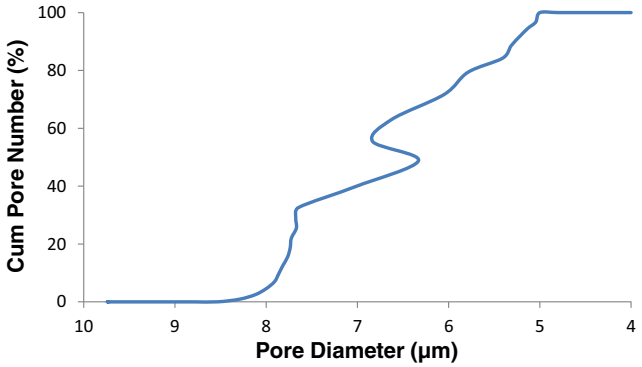

Fig. 13 Porosity distribution for an electrospun mat synthesized with an applied voltage of 20 kV

Figure 11 illustrates that SEM micrographs of PSf surfaces prepared with different electrospinning voltages for 15 wt% PSf concentration (a, b) and 25 wt% concentration (c, d) reveal negligible change of the resultant morphology with voltage increase from 17 to 26 kV. Figure 12 shows that electrospinning voltage has an insignificant influence on the contact angle for surfaces prepared with 15 % and 25 % PSf concentrations.

The electrospun mats were found to be quite porous, with the mean pore size ranging from 3 to 8 microns. This is expected, due to the fact that it consists of fibers stacked on top of each other with plenty of open spaces (about 77 %). The results for different samples show an absence of a definite trend, as none of the parameters were found to have a certain influence on the porosity characteristics. Figure 13 shows the pore size distribution for a polysulfone mat prepared with a feed concentration of 25 % under an applied voltage of 20 kV.

The thickness of the mats is also an important parameter to be considered, as it has an influence on several characteristics such as visible light transmissivity, mechanical strength, etc. Figure 14a shows the variation of thickness with feed rate for a 25 % PSf solution under an applied voltage of 20 kV. The plot shows the thickness increased almost linearly with the feed rate. The thickest mat was obtained at a feed rate of 2 mL/h with a thickness value of~60 μm.

The above trend is logical, since increasing the feed rate implies a higher volume of PSf is being produced as fibers in a given time. Also, for a given voltage, one would expect the mat thickness to increase with the polysulfone concentration in the feed solution (Fig. 14b). A more concentrated solution will be expected to give a larger volume of fibers as compared to a dilute one. However, the effect of applied voltage is unclear; for the 25 % PSf solution, we observe reduced thickness at a higher voltage. In comparison, the thickness is virtually unaffected for the 30 % feed solution.

Conclusions

Polysulfone mats of varying chemistries were fabricated by electrospinning a solution in dimethylformamide (DMF). The influence of different processing parameters, such as solution concentration, applied voltage and the feed rate on the surface morphology and wettability of the electrospun mats, was investigated. The results illustrate that the structure of the fabricated surface depends primarily on the PSf solution concentration. Three types of surface morphologies were obtained by varying the PSf concentration: beads, beads-on-strings, and free-beads fibers structures. It was found that the surface hydrophobicity depends mainly on the resultant morphology, and the existence of beads increased surface roughness and hence the measured CA. The formation of beads structure from the diluted solution can be related to the low viscosity of the solution resulting from fewer chain entanglements and a higher amount of solvent. Increasing the concentration lead to the formation of beads-on-string and free-beads fibers morphologies, which were accompanied by a decrease in CA. Before reaching to uniform free-beads fiber, the beads change from spherical to spindle-like with rising PSf concentration. The average diameters of free-beads fibers increased with increasing PSf concentration and electrospinning feed rate, while negligible change in the surface structure, and hence in the measured contact angle, was observed with varying the electrospinning voltage.

Superhydrophobic PSf surfaces with static water contact angles in excess of 150° and a contact angle hysteresis of less than 10° were successfully prepared from solutions containing 5 % and 10 % PSf concentration. However, it is worth mentioning that even surfaces with WCA<150° exhibited a hysteresis less than 10°, which makes them potential candidates for self-cleaning applications. In fact, the mechanical integrity of the fibrous morphology associated with higher PSf

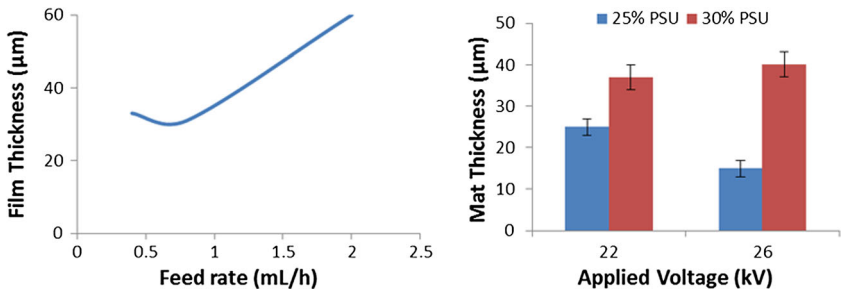

Fig. 14 Mat thickness as a function of different parameters: (**a**) feed rate, (**b**) applied voltage

concentrations makes them more feasible candidates for practical applications as compared to the beads-only structure.

To conclude, this study presents a simple approach to synthesize extremely water repellent and self-cleaning surfaces from a not very hydrophobic material, just by manipulating the surface morphology and roughness. This may be very attractive for novel industrial and practical applications that require self-cleaning. The electrospinning technique seems to be advantageous compared to contemporary techniques that are time-consuming, expensive, and/or nonversatile. Future studies should be directed towards improving the optical transparency and visible light transmissivity to expand the scope of potential applications to solar cells, PV panels, etc.

Acknowledgments The authors acknowledge the financial support of King Fahd University of Petroleum and Minerals (KFUPM) through KFUPM-MIT Project No. R16-DMN-11, and King Abdulaziz City for Science and Technology (KACST) through Project No. 11-ADV2134-04. In addition, the following personnel at KFUPM are acknowledged for their assistance with specimen preparation and characterization: Feras Kafiah for sample preparation, Prof Tahar Laoui (ME dept.) for permission to use his Nanotechnology Lab and relevant consumables, and Faheem Patel for assisting with the porosity measurements.

References

1. Zhang X, Shi F, Niu J, Jiang Y, Wang Z (2008) Superhydrophobic surfaces: from structural control to functional application. J Mater Chem 18:621–633
2. Zheng J, He A, Li J, Xu J, Han CC (2006) Studies on the controlled morphology and wettability of polystyrene surfaces by electrospinning or electrospraying. Polymer 47:7095–7102
3. Wang L, Yang S, Wang J, Wang C, Chen L (2011) Fabrication of superhydrophobic TPU film for oil–water separation based on electrospinning route. Mater Lett 65:869–872
4. Neinhuis C, Barthlott W (1997) Characterization and distribution of water-repellent, self-cleaning plant surfaces Ann. Bot 79:667–677
5. Zhan N, Li Y, Zhang C, Song Y, Wang H, Sun L, Yang Q, Hong X (2010) A novel multinozzle electrospinning process for preparing superhydrophobic PS films with controllable bead-on-string/microfiber morphology. J Colloid Interface Sci 345:491–495
6. Jiang L, Zhao Y, Zhai J (2004) A Lotus-Leaf-like Superhydrophobic Surface: A Porous Microsphere/Nanofiber Composite Film Prepared by Electrohydrodynamics. Angew Chem Int Ed 43:4338–4341
7. Chen Y, Kim H (2009) Preparation of superhydrophobic membranes by electrospinning of fluorinated silane functionalized poly(vinylidene fluoride). Appl Surf Sci 255:7073–7077
8. Lim J-M, Yi G-R, Moon JH, Heo C-J, Yang S-M (2007) Superhydrophobic Films of Electrospun Fibers with Multiple-Scale Surface Morphology. Langmuir 23:7981–7989
9. Wang H-S, Fu G-D, Li X-S (2009) Functional Polymeric Nanofibers from Electrospinning. Recent Pat Nanotechnol 3:21–31
10. Zhang L, Liu L, Pan FL, Wang D, Pan Z, Effects of Heat Treatment on the Morphology and Performance of PSf Electrospun Nanofibrous Membrane, J. Engr. Fibers & Fabrics 16, SPECIAL ISSUE - July 2012
11. Khan Z, Kafiah FM (2013) "Preparation of Polysulfone Electrospun Nanofibers: Effect of Electrospinning and Solution Parameters", Conference on Membrane Science & Technology MST, Aug. 27–29, Kaula Lumpur, Malaysia
12. Jalili R, Hosseini SA, Morshed M (2005) The Effects of Operating Parameters on the Morphology of Electrospun Polyacrilonitrile Nanofibres. Iran Polym J 14:1074
13. Fong H, Chun I, Reneker DH (1999) Beaded nanofibers formed during electrospinning. Polymer 40:4585
14. Chang KH, Lin HL (2009) Nano hydroxyapatite–polysulfone coating on Ti-6Al-4V substrate by electrospinning. J Polym Res 16:611
15. Dhakate SR, Singla B, Uppal M, Mathur RB (2010) Effect of Processing Parameters on Morphology and Thermal Properties Of Electrospun Polycarbonate Nanofibers. Adv Mat Lett 1:200
16. Cassie ABD, Baxter S (1944) Wettability of porous surfaces. Trans Faraday Soc 40:546–551
17. K. Acatay, E. Simsek, C.O.-Yang, Y.Z. Menceloglu, Tunable superhydrophobically stable polymeric surfaces by electrospinning, Angew. Chem. Int. Ed. 43 (2004) 5210–5213
18. Chen W, Fadeev AY, Hsieh MC, Oner D, Youngblood J, McCarthy TJ (1999) Ultrahydrophobic and Ultralyophobic Surfaces: Some Comments and Examples. Langmuir 15(10):3395–3399
19. Öner D, McCarthy TJ (2000) Ultrahydrophobic Surfaces. Effects of Topography Length Scales on Wettability. Langmuir 16(20):7777–7782
20. Yabu H, Shimomura M (2005) Single-Step Fabrication of Transparent Superhydrophobic Porous Polymer Films. Chem Mater 17:5231
21. Gu G, Dang H, Zhang Z, Wu Z (2006) Fabrication and characterization of transparent superhydrophobic thin films based on silica nanoparticles. Appl Phys A 83:131
22. Hozumi A, Takai O (1998) Preparation of silicon oxide films having a water-repellent layer by multiple-step microwave plasma-enhanced chemical vapor deposition. Thin Solid Films 334:54
23. Feng L, Zhang Y, Xi J, Zhu Y, Wang N, Xia F, Jiang L (2008) Petal effect: A superhydrophobic state with high adhesive force. Langmuir 24:4114
24. Duparré A, Flemming M, Steinert J, Reihs K (2002) Optical coatings with enhanced roughness for ultrahydrophobic, low-scatter applications, Appl. Opt. 41 3294
25. Tadanaga K, Kitamuro K, Matsuda A, Minami TJ (2003) Formation of Superhydrophobic Alumina Coating Films with High Transparency on Polymer Substrates by the Sol–gel Method, Sol–Gel Sci. Technol 26:705
26. Rao AV, Latthe SS, Nadargi DY, Hirashima H, Ganesan V (2009) Preparation of MTMS based superhydrophobic silica films by sol–gel method. J Colloid Interface Sci 332:484
27. Quere D, Lafuma A, Bico J (2003) Slippy and sticky microtextured solids. Nanotechnology 14:1109
28. Lafuma A, Quere D (2003) Superhydrophobic states. Nat Mater 2:457